

Anisotropic flows from initial state of a fast nucleus

K.G. Boreskov, A.B. Kaidalov, O.V. Kancheli

*Institute for Theoretical and Experimental Physics,
Moscow, 117218 Russia*

Abstract

We analyze azimuthal anisotropy in heavy ion collisions related to the reaction plane in terms of standard reggeon approach and find that it is nonzero even when the final state interaction is switched off. This effect can be interpreted in terms of partonic structure of colliding nuclei. We use Feynman diagram analysis to describe details of this mechanism. Main qualitative features of the appropriate azimuthal correlations are discussed.

Introduction

Investigations of azimuthal anisotropy of secondary particle distributions in heavy ion collisions is used as an effective tool for analysis of dynamical mechanisms of these processes. Anisotropic flows and, in particular, the elliptic flow $v_2 \equiv \langle \cos 2\phi \rangle$ are considered usually as an important source of information about properties of a dense state of hadronic matter formed in the anisotropic overlap region of colliding nuclei¹. Crucial point is the relation of the anisotropy to the reaction plane orientation (azimuthal correlations not related to this orientation are called non-flow correlations). The dependencies of flow coefficients on c.o.m. energy, centrality, rapidity and transverse momentum of secondaries are ascribed usually to anisotropic properties of strongly interacting matter at early times after collision. It is assumed that anisotropic flows are due to final state interactions and in hydrodynamic models originate from pressure gradients connected to original asymmetry in the configuration space for noncentral collisions. Practically all existing models for anisotropic flows use classical description of processes.

In this paper we use quantum relativistic approach, based on analysis of Feynman diagrams and reggeon diagrams for a study of anisotropic flows in collisions of hadrons and nuclei at high energies. We show that a part of azimuthal anisotropy can be related to properties of *initial* state of a fast nucleus. Namely, we analyze azimuthal correlations present in partonic configurations of fast colliding nuclei. Thus a part of the observed azimuthal asymmetry of final particles can come from parton correlations in initial state. We demonstrate how anisotropic flows in this case are related to the anisotropy of the overlap region.

¹See e.g. [1] - [8].

It is worth to point out that, though it is not possible to measure in general both transverse momenta and transverse coordinates of partons, but for fast moving heavy nucleus impact parameters of nucleons and fast partons can be fixed with a good accuracy. Therefore for colliding nuclei the radial directions in every point of transverse plane with respect to c.o.m. are well defined. Distributions of partons at each point are anisotropic in general. The collision process (if it is not absolutely central) selects partonic configurations asymmetric in impact parameter plane. This transforms the initial ‘radial’ asymmetry in colliding nuclei to the azimuthal asymmetry of produced particles momenta with respect to the collision plane.

The simplest way to study such phenomena theoretically is to use the reggeon diagrams for inclusive cross sections, where all details of parton interactions are encoded in vertices and Regge trajectories – and we follow this way in the paper.

The paper ² is organized as follows. In Sec.1 we calculate a contribution to v_2 due to standard multiperipheral production described by reggeon diagram for inclusive production. The calculation is carried out in the momentum representation and gives v_2 as a function of impact parameter \mathbf{b} and particle transverse momentum \mathbf{p}_t . A simple phenomenological parameterization is used for the vertex of a detected particle emission. Then in Sec.2 we give a qualitative interpretation of the results in terms of the impact plane analysis. It is shown that the obtained azimuthal asymmetry can be ascribed to specific correlations presented at the level of partonic configuration of wave function of the fast nucleus. It exists without any final state interactions, which are usually considered as an obligatory condition for appearance of correlations related to the reaction plane orientation. We explain how these primary correlations manifest themselves as the elliptic flow due to anisotropy of the overlap region. In Sec.3 we make an estimate of the anisotropy structure of the inclusive vertex in simple multiperipheral models and show that they naturally result in azimuthal dependence. Possible mechanisms enhancing the effect are discussed. In Sect.4 we discuss generation of the directed flow effect in the same model. This effect is produced by nondiagonal in reggeons RP vertex and therefore it is concentrated at edges of rapidity space. In Sec.5 we discuss contribution to 2-particle azimuthal correlations in reggeon approach and suggest possible tests of this mechanism. Sec.6 contains discussion of multipomeron interactions which can have crucial influence on magnitude of the effect and on its atomic number and impact parameter dependencies. In Sec.7 numerical estimates are presented to illustrate main qualitative features of the model. In Sec.8 we briefly summarize our main results.

1 Momentum representation

Let us explain first the mechanism under consideration using reggeon diagrams. A simplest way to produce secondary particles at high energy is given by multiperipheral diagram of Fig.1a. Inclusive cross section is described by the reggeon diagram of Fig.1b which corresponds to squared multiparticle amplitude with fixed momentum p of a single detected particle.

Single particle inclusive cross section is related to the amplitude $G(\mathbf{q}, \mathbf{p})$ of the diagram

² This paper is an extended version of a talk given at Session of Nuclear Physics Division of Russian Academy of Sciences in November 2007.

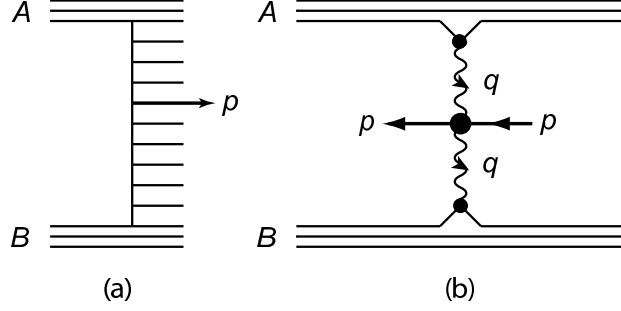


Figure 1: Reggeon diagram for one-particle inclusive production

of Fig.1b at zero transfer momentum $\mathbf{q} = 0$:

$$F_{incl}(\mathbf{p}_t; y) \equiv \frac{d\sigma}{d^2\mathbf{p}_t dy} \sim G(\mathbf{q} = 0; \mathbf{p}_t, y) , \quad (1)$$

where p_t and y are transverse momentum and rapidity of the registered particle. We, however, need to calculate a contribution of this diagram at various values of \mathbf{q} in order to find a correlation between transverse momentum \mathbf{p}_t and impact parameter value for colliding nuclei, \mathbf{b} . This relation is given by Fourier transform of $G(\mathbf{q}; \mathbf{p}_t, y)$

$$\tilde{F}_{incl}(\mathbf{p}_t, y; \mathbf{b}) \sim \tilde{G}(\mathbf{b}; \mathbf{p}_t, y) = \int \frac{d^2\mathbf{q}}{(2\pi)^2} e^{i\mathbf{b}\mathbf{q}} G(\mathbf{q}; \mathbf{p}_t, y) . \quad (2)$$

Here

$$G(\mathbf{q}; \mathbf{p}_t, y) = F_A(q)D(\mathbf{q}; y)\gamma(\mathbf{q}, \mathbf{p}_t)D(\mathbf{q}; Y - y)F_B(q) , \quad (3)$$

where $F_{A,B}$ are 2-dimensional form factors of colliding nuclei which are Fourier transforms of their 2-dimensional profiles, $T_{A,B}(b)$,

$$F_{A,B}(q) = \int d^2b e^{-i\mathbf{q}\mathbf{b}} T_{A,B}(b) , \quad F_A(0) = A, \quad F_B(0) = B, \quad (4)$$

and functions $D(\mathbf{q}; y), D(\mathbf{q}; Y - y)$ are connected to s-channel discontinuities of reggeon amplitudes (“cut reggeons”) ³

$$D(\mathbf{q}; y) \equiv 2 \text{Im}f(\mathbf{q}; y) = g_N e^{-(R_0^2 + \alpha' y)q^2} e^{[\alpha(0) - 1]y} . \quad (5)$$

An inclusive vertex of the reggeon diagram $\gamma(\mathbf{q}, \mathbf{p}_t)$ depends on 2-dimensional momenta \mathbf{p}_t and \mathbf{q} . For estimates we will use the phenomenological parametrization

$$\gamma(\mathbf{q}, \mathbf{p}_t) = \gamma_0 \exp\{-r_q^2 \mathbf{q}^2 - r_p^2 \mathbf{p}_t^2 - \epsilon r_0^4 (\mathbf{p}_t \mathbf{q})^2\} . \quad (6)$$

Here dimensional coefficients r_q, r_p are expected to be of typical hadronic sizes about $r_0 = 1$ fm, and ϵ of order of 1.

The dependence on variable $(\mathbf{p}_t \mathbf{q})$ is crucial for appearance of azimuthal correlations typical for elliptic flow. Note that the terms proportional to the odd powers of $\mathbf{p}_t \mathbf{q}$ should

³We use an exponential parameterization of reggeon vertex $g_N \exp(-R_0^2 \mathbf{q}^2)$ and linear Regge trajectory $\alpha(\mathbf{q}^2) = \alpha(0) - \alpha' \mathbf{q}^2$.

be absent if both reggeons have positive C -parity (like pomerons) because the vertex should be even under the change $\mathbf{p}_t \rightarrow -\mathbf{p}_t$. More detailed analysis of structure and value of the vertex $\gamma(\mathbf{q}, \mathbf{p}_t)$ will be performed in sections 3,4.

The elliptic flow v_2 is defined as a second Fourier coefficient in an azimuthal dependence of inclusive spectrum

$$\frac{d\sigma}{dp_t^2 d\phi} \propto 1 + \sum_1^{\infty} 2v_n(b; p_t, y) \cos(n\phi) , \quad (7)$$

where ϕ is an azimuthal angle between impact parameter \mathbf{b} which determines the reaction plane and transverse momentum \mathbf{p}_t . Thus,

$$v_2(b; p_t, y) \equiv \frac{C_2}{C_0} = \frac{\int d\phi \cos(2\phi) G(\mathbf{b}; \mathbf{p}_t, y)}{\int d\phi G(\mathbf{b}; \mathbf{p}_t, y)} . \quad (8)$$

For the vertex function parameterized by eq.(6) one gets

$$C_n(b; p_t, y) = \int qdq J_n(bq) F_A(q^2) F_B(q^2) D(q; y) D(q, Y - y) c_n(q; b, p_t) , \quad n = 0, 2, \quad (9)$$

with

$$\begin{aligned} C_0(q; b, p_t) &= I_0(\epsilon r_0^4 p_t^2 q^2 / 2) e^{-\epsilon r_0^4 p_t^2 q^2 / 2} , \\ C_2(q; b, p_t) &= I_2(\epsilon r_0^4 p_t^2 q^2 / 2) e^{-\epsilon r_0^4 p_t^2 q^2 / 2} . \end{aligned} \quad (10)$$

where I_0, I_1 are the modified Bessel functions.

To estimate an order of the effect let us first make the calculation with the approximate Gaussian parameterization of nuclear form factors $F_{A,B}(q^2)$:

$$F_{A,B}(q^2) = \exp(-R_{A,B}^2 q^2 / 4) . \quad (11)$$

Then

$$v_2(b; p_t, y) = \frac{I_2(\alpha/2)}{I_0(\alpha/2)} \quad (12)$$

with

$$\alpha = \frac{\epsilon r_0^4 p_t^2 b^2}{R^2 (R^2 + 4\epsilon r_0^4 p_t^2)} , \quad R^2 = R_A^2 + R_B^2 + R_{regge}^2(Y) . \quad (13)$$

For $\alpha \ll 1$ we have :

$$v_2 \simeq \frac{\alpha}{4} \simeq \epsilon (r_0 p_t)^2 \left(\frac{r_0}{R} \right)^2 \left(\frac{b}{2R} \right)^2 . \quad (14)$$

Thus, v_2 is proportional to the ‘‘ellipticity’’ ϵ of the inclusive vertex γ . The sign of v_2 is the same as the one of ϵ which can be both positive and negative depending on dynamical structure of the inclusive vertex (see discussion in Sect.3). The formula (14) reveals an increase of v_2 with transverse momentum \mathbf{p}_t and impact parameter b . Results of numerical calculations are presented in sec.7.

2 Impact parameter representation

Presentation of formulas in terms of impact parameters allows us to give more instructive interpretation of the results. Eqs.(2),(3) in these variables have the form:

$$G(\mathbf{b}; \mathbf{p}_t, y) \sim \int d^2\boldsymbol{\beta}_1 \int d^2\mathbf{b}_1 \int d^2\mathbf{b}_2 \int d^2\boldsymbol{\beta}_2 T_A(\boldsymbol{\beta}_1) t_1(\mathbf{b}_1 - \boldsymbol{\beta}_1; y) \\ \times \Gamma(\mathbf{b}_2 - \mathbf{b}_1, \mathbf{p}_t) t_2(\boldsymbol{\beta}_2 - \mathbf{b}_2; Y - y) T_B(\mathbf{b} - \boldsymbol{\beta}_2) . \quad (15)$$

Here (see Fig.2) $\boldsymbol{\beta}_1$ and $\mathbf{b} - \boldsymbol{\beta}_2$ are the positions of participant nucleons of the nuclei A and B with nuclear profiles T_A and T_B , $t(\boldsymbol{\beta}; y)$ is a Fourier transform of reggeon propagator $D(\mathbf{q}; y)$ and $\Gamma(\mathbf{b}; \mathbf{p}_t)$ is a Fourier transform of the inclusive vertex $\gamma(\mathbf{q}, \mathbf{p}_t)$:

$$\Gamma(\mathbf{b}; \mathbf{p}_t) = \int \frac{d^2\mathbf{q}}{(2\pi)^2} e^{i\mathbf{q}\mathbf{b}} \gamma(\mathbf{q}, \mathbf{p}_t) . \quad (16)$$

For the exponential model approximation (6), one has

$$\Gamma(\mathbf{b}; \mathbf{p}_t) = \frac{\pi e^{-r_b^2 p_t^2}}{\sqrt{r_q^2(r_q^2 + \epsilon r_0^4 p_t^2)}} \exp\left(-\frac{b_x^2}{4(r_q^2 + \epsilon r_0^4 p_t^2)} - \frac{b_y^2}{4r_q^2}\right) , \quad (17)$$

where b_x is a component of \mathbf{b} along \mathbf{p}_t and b_y in the transverse direction. In order to reveal

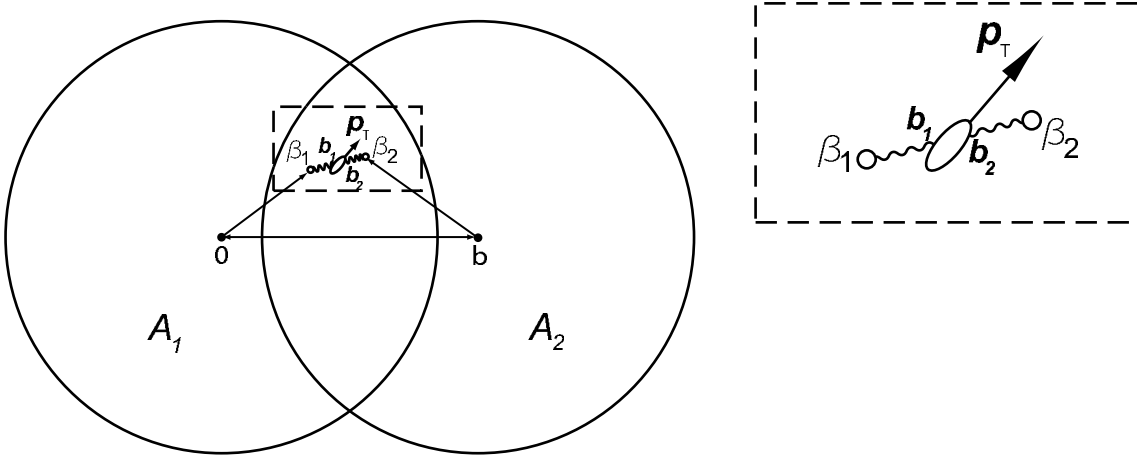


Figure 2: Interaction of two nucleons in impact plane

a structure of Eq.(15) it can be written symbolically as a number of convolutions with notation $f \otimes g$ for convolution of functions f and g :

$$F_{incl}(\mathbf{p}_t, y; \mathbf{b}) \sim T_A \otimes t(y) \otimes \Gamma \otimes t(Y - y) \otimes T_B . \quad (18)$$

Convolutions in eq.(15) can be done in arbitrary order, so it is equivalent to

$$F_{incl}(\mathbf{p}_t, y; \mathbf{b}) \sim T_{int} \otimes \Gamma = \int d^2\mathbf{a} T_{int}(\mathbf{b} - \mathbf{a}) \Gamma(\mathbf{a}; p_t) . \quad (19)$$

Here the function T_{int} which characterize a region of interaction of nuclei in \mathbf{b} space is a convolution of the nuclear overlap ⁴ $T_{AB} = T_A \otimes T_B$ and combined reggeon amplitude t_{regge} :

$$T_{int} = T_{AB} \otimes t_{regge} ,$$

where

$$t_{regge}(b; Y) = t(y) \otimes t(Y - y) = \frac{g_N^2}{4\pi R_{regge}^2(Y)} \exp\left(-\frac{b^2}{4R_{regge}^2(Y)}\right) ,$$

$$R_{regge}^2(Y) = 2R_0^2 + \alpha' Y ,$$

describes the reggeon-interaction amplitude of nucleons from colliding nuclei.

For Gaussian parameterization of nuclear profiles T_A, T_B all convolutions have the Gaussian form again, resulting in the same final answer (12).

In the impact parameter representation it is easy to see an origin of the correlation between directions of \mathbf{b} and transverse momentum \mathbf{p}_t . Registration of the inclusive particle is realized by nonlocal probe which structure is determined by the inclusive vertex $\Gamma(\mathbf{b}; \mathbf{p}_t)$. This vertex has an elliptic anisotropy in b -plane along the direction of \mathbf{p}_t (see examples in Sec.3). Due to this anisotropy the convolution of the overlap function T_{int} and Γ is sensitive to gradients of nuclear densities.

The size of the probe range is small in comparison to nuclear size $R_A \sim R_B \sim A^{1/3}r_0$, so it is possible to calculate the integral (19) expanding the smooth distribution $T_{int}(\mathbf{b}-\mathbf{a})$ over small corrections $a_x/R_A, a_y/R_A$. After integration over a_x, a_y we get explicitly anisotropic expression for the inclusive cross section (recall that the axis x is chosen along the momentum \mathbf{p}_t). Omitting higher order terms in a_i/R_A we have in the approximation (6),(17)

$$F_{incl} \sim T_{int}(b^2) + 2(2r_q^2 + \epsilon r_0^4 p_t^2) \frac{dT_{int}(b^2)}{d(b^2)} + 4 \frac{d^2 T_{int}(b^2)}{d(b^2)^2} [(r_q^2 + \epsilon r_0^4 p_t^2) b_x^2 + r_q b_y^2] , \quad (20)$$

where derivatives are taken over the variable b^2 . Thus, for the elliptic flow coefficient we have

$$v_2 \simeq \epsilon \frac{r_0^4 T_{int}''(b^2)}{T_{int}(b^2)} \mathbf{p}_t^2 \mathbf{b}^2 . \quad (21)$$

The second derivative of $T_{int}(\mathbf{b}^2)$ contains a small parameter of order of $(r_0/R_A)^4$ which appears explicitly in Eq.(14).

This formula can be interpreted in terms of parton probe. The local probe feels only parton density. An information about density gradients and its higher derivatives can be obtained by means of nonlocal probes with typically hadronic range. Being restricted only with lower multipoles a structure of the probe can be written as

$$\Gamma(\mathbf{a}; \mathbf{p}) \sim (1 + \bar{\delta} p_i \partial_i + (\beta \delta_{ij} + \bar{\epsilon} p_i p_j) \partial_i \partial_j + \dots) \delta^{(2)}(\mathbf{a}) , \quad (22)$$

where $\partial_i = \partial/\partial a_i$ and $\bar{\delta} \equiv \delta r_0^2$, $\bar{\epsilon} \equiv \epsilon r_0^4$ are dimensional coefficients of typical hadronic range. The first term measures parton density as well as the isotropic one with δ_{ij} , the second term

⁴ To avoid confusion let us stress that T_{AB} describes how the number of nucleons from colliding nuclei which overlap in the impact plane depends on collision impact parameter b . It is an isotropic function not depending on the vector \mathbf{b} direction.

feels gradients, and the ϵ -term gives an information about ellipticity of partonic distribution at the point of production of registered particle. So the distribution over transverse momenta turns out to be correlated with impact parameter \mathbf{b} :

$$\begin{aligned}
F_{incl}(\mathbf{p}_t; \mathbf{b}) &\sim T_{int} \otimes \Gamma = \int d^2\mathbf{a} T_{int}(\mathbf{b} - \mathbf{a}) \Gamma(\mathbf{a}; \mathbf{p}_t) \\
&\approx T_{int}(b^2) + \bar{\delta} p_{ti} \partial_i T_{int}(b^2) + \bar{\epsilon} p_{ti} p_{tj} \partial_i \partial_j T_{int}(b^2) \\
&\approx T_{int}(b^2) + 2\bar{\delta}(\mathbf{p}_t \mathbf{b}) T'_{int}(b^2) + 4\bar{\epsilon}(\mathbf{p}_t \mathbf{b})^2 T''_{int}(b^2), \tag{23}
\end{aligned}$$

where T' denotes the derivative over b^2 . This reproduces the elliptic flow coefficient $v_2 = \epsilon(\mathbf{p}_t \mathbf{b})^2 T''_{int}(b^2)$ (cf. with (21)). The δ -term corresponds to the first flow coefficient $v_1 = \delta(\mathbf{p}_t \mathbf{b}) T'_{int}(b^2)$ (directed flow), which we discuss in Sec. 4.

Let us stress that partonic interpretation of reggeon diagrams depends on chosen Lorentz frame. Reggeon exchanges are highly non-local in space-time due to their complicated multiparticle internal structure. From this viewpoint the fast hadron or nucleus is essentially a multiparton state of multiperipheral configuration (Fig.1a represents the simplest example). The particles of such configuration are ordered in their rapidities and only most slow particles interact with a target. This means that in the lab frame related to the nucleus B the nucleus A is a multiparton state containing the detected particle with rapidity y and transverse momentum \mathbf{p}_t among others. This state has already an anisotropy in partonic distributions due to correlation between parton transverse momentum \mathbf{p}_t and its position \mathbf{b}_1 in impact parameter plane. If nuclear collision is central then the overlap region is isotropic and after integration over b_1 anisotropy disappears. At non-central collision, however, the overlap region has anisotropic almond shape and integration over this region keeps anisotropic distribution in \mathbf{p}_t .

3 Inclusive vertex

Let us estimate in simple models an anisotropy of inclusive \mathbf{p}_t probe related to the vertex $\gamma(\mathbf{q}, \mathbf{p}_t)$. If multiperipheral ladder of Fig.1 consists of scalar particles with triple coupling then a structure of inclusive vertex is determined in lowest order by Fig.3 where momentum \mathbf{p}_t is fixed. Then the vertex can be written as 2-dimensional integral ⁵

$$\gamma(\mathbf{q}, \mathbf{p}_t) = g^2 \int d^2\mathbf{k} G(\mathbf{k}) G(\mathbf{k} - \mathbf{p}_t) G(\mathbf{q} - \mathbf{k}) G(\mathbf{q} - \mathbf{k} + \mathbf{p}_t), \tag{24}$$

where particle propagators G depend on 2-dimensional momenta only.

To estimate an anisotropy effect let us consider the vertex γ at small $q \sim p_t \ll \mu$ (here $\mu \sim r_0^{-1}$ is a typical mass parameter):

$$\gamma(p_t, q, z) \simeq \gamma(p_t^2) \left(1 - \epsilon \frac{q^2 p_t^2}{\mu^4} z^2 + \dots \right), \tag{25}$$

⁵ There is an integration over 3-dimensional momentum \mathbf{k} in the loop but for estimate we shall assume that longitudinal integration is already carried out. It introduces t_{min} terms into propagators which can be replaced by change of effective masses. So, in what follows we use propagators as functions of 2-dimensional momenta.

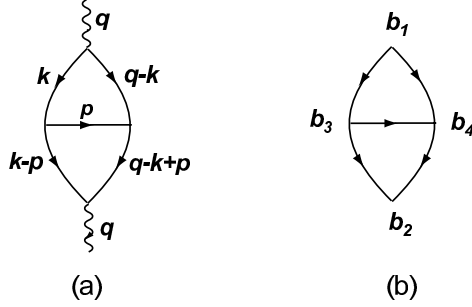


Figure 3: Simplest inclusive reggeon vertex

where $z = \cos \phi$ is a cosine of the angle between \mathbf{p}_t and \mathbf{q} . The coefficient which determines a degree of ellipticity is denoted as ϵ as we did before. For standard perturbative behavior of propagators: $G(\mathbf{k}) = (\mathbf{k}^2 + \mu^2)^{-1}$ numerical estimate gives a value $\epsilon \approx -0.2$ for scalar couplings g in the diagram 3. Note that such a sign corresponds to negative v_2 (in contrast to experimental observation). This fact can be understood in a simple way by writing Eq.(24) in coordinate representation (see Fig.3b):

$$\begin{aligned} \tilde{\gamma}(\mathbf{b}_{12}, \mathbf{b}_{34}) = & g^2 \int \prod_i d^2 \mathbf{b}_i \tilde{G}(b_{13}) \tilde{G}(b_{32}) \tilde{G}(b_{24}) \tilde{G}(b_{41}) \\ & \times \delta^2(\mathbf{b}_{12} - (\mathbf{b}_2 - \mathbf{b}_1)) \delta^2(\mathbf{b}_{34} - (\mathbf{b}_4 - \mathbf{b}_3)) , \end{aligned} \quad (26)$$

where $\mathbf{b}_{ij} = \mathbf{b}_i - \mathbf{b}_j$, and the vector \mathbf{b}_{12} is conjugated to \mathbf{q} , while \mathbf{b}_{34} – to the momentum \mathbf{p}_t . The 2-dimensional Green functions $\tilde{G}(\mathbf{b}) \sim \exp(-\mu|\mathbf{b}|)$ and therefore the integrand in (26) depends only on sum of all lengths $|\mathbf{b}_{13}| + |\mathbf{b}_{32}| + |\mathbf{b}_{24}| + |\mathbf{b}_{41}|$. It can be seen purely geometrically that maximum of $\prod \tilde{G}$ at fixed $|\mathbf{b}_{34}|, |\mathbf{b}_{12}|$ is reached in the configuration with parallel \mathbf{b}_{12} and \mathbf{b}_{34} . The maximal anisotropy (~ 0.3) corresponds to $|\mathbf{b}_{12}|/|\mathbf{b}_{34}| \sim 1$ and decrease strongly with change of this ratio. Since $\gamma(\mathbf{b}_{12}, \mathbf{b}_{34})$ is maximal for parallel \mathbf{b}_{12} and \mathbf{b}_{34} , then $\gamma(\mathbf{q}, \mathbf{p}_t)$ is maximal at parallel \mathbf{q} and \mathbf{p}_t , i.e. ϵ is negative. Similar arguments can be generalized to more complicated diagrams with spinless particles – configurations with parallel \mathbf{b}_{12} and \mathbf{b}_{34} are more probable.

The value and the sign of the effect depend on dynamical structure of the inclusive vertex $\gamma(\mathbf{q}, \mathbf{p}_t)$ – on form of propagators⁶ and, more important, on structure of vertex of particle emission. Vertex properties are very sensitive to particle spin because it gives an extra azimuthal dependence. Calculations show that if the inclusive particle has spin 1 (see, Fig.4), then the sign of ϵ is different (in accordance with data) and its value increases. Note that such situation is not far from reality because ρ -mesons give a considerable part of multiperipheral particles and pions due to their decays have mainly close transverse momenta. Numerical estimate gives $\epsilon \sim 0.5$.

Properties of the inclusive vertex $\gamma(\mathbf{q}, \mathbf{p}_t)$ can be studied experimentally in NN collisions, for instance by analysis of azimuthal two-particle correlations for hadrons in different windows of rapidity values.

Let us discuss behaviour of the inclusive vertex $\gamma(\mathbf{q}, \mathbf{p}_t)$ at large p_t . In region $\mathbf{p}_t^2 \gg \mu^2$ it should decrease according to perturbation theory in power-like way, $\sim (\mu/p_t)^m$, where

⁶ Note that in case of Gaussian form of propagators, $G(k) = \exp(-k^2/\mu^2)$, the product of propagators in coordinate space does not depend on the angle resulting in zero anisotropy, $\epsilon = 0$.

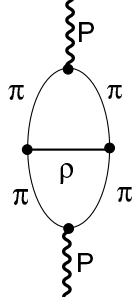


Figure 4: PP -diagram for inclusive ρ -meson production

a degree m depends on dynamics. In simple scalar theory (24) $\gamma(\mathbf{q}, \mathbf{p}_t) \sim (\mu/p_t)^4$, and z -depending coefficients decrease even faster, leading to a small ellipticity:

$$|\epsilon(p_t)| = \left| \frac{\gamma(q^2, p_t^2, z=1) - \gamma(q^2, p_t^2, z=0)}{\gamma(q^2, p_t^2, z=1)} \right| \sim (\mu/p_t)^2 \quad \text{at } p_t^2 \gg \mu^2.$$

It means that a size of the p_t -probe becomes much smaller than μ^{-1} and its form becomes more isotropic ⁷.

The situation is different if the vertex includes particles with spin because in this case spin terms give an additional z dependence. As an example, in case of inclusive production of vector particles explicit calculation gives non-vanishing vertex ellipticity, $\epsilon(p_t) \rightarrow \text{const}$ when $p_t^2 \gg \mu^2$.

4 Directed flow

The mechanism applied to generation of the elliptic flow v_2 contributes to all v_n -harmonics. As it was mentioned in Sec.1 there is a peculiarity related to odd harmonics – the PP reggeon diagram do not contribute there because of symmetry of the PP inclusive vertex. The odd harmonics appear for vertices which couple different types of reggeons (RP vertices where R is a secondary reggeon, e.g. ρ).

Consider as an example contribution of diagrams of Fig.5 to the first harmonic corresponding to the directed flow v_1 . These diagrams contain the rapidity dependent factor which comes from the reggeon propagator $D_R(\mathbf{q}, y) \sim \exp(\Delta_\rho y)$ where $\Delta_\rho \approx 0.5$. The diagrams (a) and (b) have different sign for the term $\mathbf{q}\mathbf{p}_t$ so for the rapidity changing in the interval $[-Y, Y]$ we get a factor $f_\rho(y) = 2 \exp(-\Delta_\rho Y) \sinh(\Delta_\rho y)$.

We have to compare the term in $\gamma^{(RP)}$ proportional to $\mathbf{q}\mathbf{p}_t$ with the angle independent term $\gamma(\mathbf{p}_t, \mathbf{q} = 0)$ due to main diagram of Fig. 1b (see Eq.(24)). For small \mathbf{p}_t

$$\gamma_1^{(RP)}(\mathbf{q}, \mathbf{p}_t)/\gamma(\mathbf{p}_t, \mathbf{q} = 0) \simeq \frac{\delta}{\mu^2} \mathbf{q}\mathbf{p}_t. \quad (27)$$

⁷ It is clearly seen in the coordinate representation (26), since $b_{12}^2 \sim \mu^{-2}$, $b_{34}^2 \sim p_t^{-2} \ll \mu^{-2}$, and the integrand depends on relative orientation of \mathbf{b}_{12} and \mathbf{b}_{34} only in high orders in (μ/p_t)

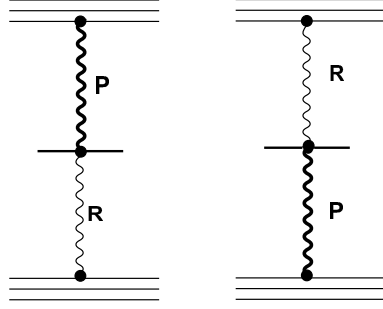


Figure 5: Inclusive reggeon-pomeron diagrams contributing to v_1 .

Calculation of the direct flow v_1 due to the RP diagrams are similar to ones made in Sect.3 and give (compare to (14))

$$v_1 \simeq \delta(r_0 p_t) \left(\frac{r_0}{R}\right) \left(\frac{b}{2R}\right) f_\rho(y) . \quad (28)$$

The numerical estimate of diagram of Fig.6 gives $\delta \sim 0.1 \div 0.5$. Qualitative behaviour of v_1 as a function of y , b and p_t is in agreement with experimental data (see Sect.7).

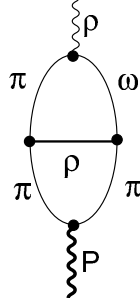


Figure 6: RP -diagram for inclusive ρ -meson production

Note also that in this model the expressions for high-order flows contain at small p_t the same parameters as v_1 and v_2 but in higher powers.

$$v_n \simeq \delta_n (r_0 p_t)^n \left(\frac{r_0}{R}\right)^n \left(\frac{b}{2R}\right)^n . \quad (29)$$

5 Two-particle azimuthal correlations

We discussed hitherto correlations of transverse momentum of the detected particle with respect to the reaction plane. The reaction plane orientation is difficult to reconstruct from experimental data, and often another method for studying anisotropic flow is used. It is related with analysis of two-particle azimuthal distributions, which contain an information on anisotropic flow. As it is seen from analysis of experimental data the main part of these correlations is related to the $\mathbf{p}_t - \mathbf{b}$ correlations for each particle. However, there

are possible sources of two-particle correlations unrelated to the reaction plane, so called ‘non-flow’ correlations.

Corresponding two-particle inclusive reggeon diagrams are shown in fig.7. To calculate anisotropic flows these diagrams should be estimated not at zero momentum transfer $\mathbf{q} = 0$ as for standard bi-inclusive cross section but at fixed value of impact parameter b .

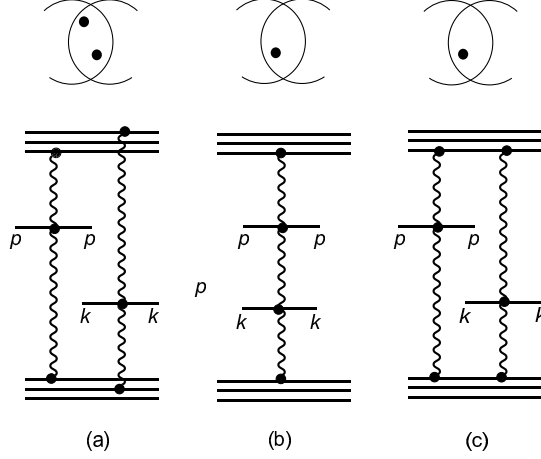


Figure 7: Reggeon diagrams for two particle inclusive production. (a) - particles p and k are emitted from different regions in transverse plane; (b) - p and k are emitted from a single reggeon chain; (c) - p and k are emitted from two reggeon chains attached to a single nucleon pair in colliding nuclei.

The contribution of the diagram 7a is factorized in the impact parameter representation and contains factors corresponding to one-particle production of Fig.1b (see (23)).

$$F_{incl}^{(a)}(\mathbf{p}_t, \mathbf{k}_t; \mathbf{b}) \sim \left[T_{int}(b^2) + 4\epsilon(\mathbf{p}_t \cdot \mathbf{b})^2 T_{int}''(b^2) \right] \left[T_{int}(b^2) + 4\epsilon(\mathbf{k}_t \cdot \mathbf{b})^2 T_{int}''(b^2) \right]. \quad (30)$$

This results in factorized formula:

$$\langle e^{2i(\phi_{p_t} - \phi_{k_t})} \rangle = \frac{\int d^2\mathbf{p}_t d^2\mathbf{k}_t e^{2i(\phi_{p_t} - \phi_{k_t})} F_{incl}(\mathbf{p}_t, \mathbf{k}_t; \mathbf{b})}{\int d^2\mathbf{p}_t d^2\mathbf{k}_t F_{incl}(\mathbf{p}_t, \mathbf{k}_t; \mathbf{b})} = v_2(p_t)v_2(k_t). \quad (31)$$

The contribution of diagram 7b is given by a convolution of T_{int} with two probes:

$$F_{incl}^{(b)}(\mathbf{p}_t, \mathbf{k}_t; \mathbf{b}) = \int d^2\mathbf{a}_1 d^2\mathbf{a}_2 T_{int}(\mathbf{b} - \mathbf{a}_1 - \mathbf{a}_2) \Gamma(\mathbf{a}_1; \mathbf{p}_t) \Gamma(\mathbf{a}_2; \mathbf{k}_t). \quad (32)$$

This distribution (in the dipole approximation (22) with $\alpha = 0$) will contain higher derivatives of T_{int} over b^2 :

$$F_{incl}^{(b)}(\mathbf{p}_t, \mathbf{k}_t; \mathbf{b}) \sim T_{int} + 8\epsilon^2(\mathbf{k}_t \cdot \mathbf{p}_t)^2 T_{int}'' + 32\epsilon^2(\mathbf{k}_t \cdot \mathbf{p}_t)(\mathbf{p}_t \cdot \mathbf{b})(\mathbf{k}_t \cdot \mathbf{b}) T_{int}^{(3)} + 8\epsilon^2(\mathbf{p}_t \cdot \mathbf{b})^2(\mathbf{k}_t \cdot \mathbf{b})^2 T_{int}^{(4)}. \quad (33)$$

All ϵ^2 -terms are at $b \sim R$ of the same order of value, $O(1)$, and are small compared to the main term in Eq.(30), which is of order $O(R^2) \sim A^{4/3}$. So extra unfactorized correction to Eq.(31) due to diagram 7b is inessential.

The situation is different for diagram 4c. Its isotropic part has a smallness of order $A^{-4/3}$ in comparison with isotropic part of $F_{incl}^{(a)}$. The anisotropic part contains a ‘non-flow’ term $(\mathbf{p}_t \cdot \mathbf{k}_t)^2$ which contains the overlap function T_{AB} (not its derivatives). As a result its contribution to (31) is of the same order as due to factorized structure $(\mathbf{p}_t \mathbf{b})^2 (\mathbf{k}_t \mathbf{b})^2$ from Eq.(30). This contribution violates factorization in Eq.(31) for two-particle correlation. Note that the ‘flow’ and ‘non-flow’ structures have different dependence on impact parameter.

6 Role of multipomeron interactions

In this section we try to estimate contributions to azimuthal asymmetry coming from multipomeron interactions. The simplest reggeon diagram of Fig.1b gives main contribution to inclusive cross section. Contributions of multipomeron diagrams of Glauber type cancel each other because of the AGK rules [9]⁸. Note that in ‘event-by-event’ analysis the number of secondary particles is fixed for every individual event, and the AGK rules may not be fulfilled. However, all extra interactions change both isotropic and anisotropic parts of the amplitude to the same extent, and therefore do not change the flow coefficients v_n .

In reggeon theory with $\alpha_P(0) > 1$ the number of pomeron exchanges increases with energy, so a role of inter-pomeron interactions grows. Detailed analysis of multipomeron effects will be published elsewhere, and here we will discuss briefly physical reasons for possible increase of azimuthal anisotropy.

When energy increases a longitudinal length of the nucleon tube with fixed transverse position is contracted and multiperipheral fluctuations connected to each of fast nucleons overlap each other in longitudinal size. Therefore a probability for particles (partons) of different chains (related to different nucleons) to interact increases. Two chains can either fuse to a single chain (triple pomeron interaction) or rescatter without changing a whole chain number (2-2 or, more generally, n - n pomeron vertices). Effects of fusion become noticeable already at RHIC energies, resulting in reduction of secondary density about two times as compared with the eikonal approximation [10]. This effect is mainly due to diagrams with three-pomeron interaction (Fig.8a). But due to their sign-alternating character a profile of the amplitude becomes more smooth and the azimuthal asymmetry becomes even smaller because of smaller gradients of parton density.

Different situation is realized for diagrams with chain rescattering (Fig. 8b) which give positive contributions to inclusive cross section. Even if the total inclusive cross section changes slightly due to such rescatterings, its anisotropic part may be strongly increased. Indeed, the expression (18) for inclusive cross section will contain in case of n interacting chains a convolution $T_A^n \otimes T_B^n$ instead of $T_A \otimes T_B$. Azimuthal asymmetry is determined by density derivatives (see (21)), therefore an extra factor $\langle n(b) \rangle^2$ will appear in expression for v_2 . The number of interacting pomerons at RHIC energies is not large ($\langle n(b) \rangle \sim 2$ for central collision), but increase of v_2 can be considerable because the effect is quadratic in n (see Fig.9 in section 7). Note that $\langle n(b) \rangle$ increases with atomic number A and changes the A dependence for v_2 also. The same mechanism may give an increase of $\langle p_t^2 \rangle$.

⁸ The cancellation occurs between diagrams with different numbers of reggeon chains (cut reggeons) considered together with sign-alternating absorptive corrections (uncut reggeons). Note that consistent account for absorptive corrections is an important feature of the reggeon approach which differs it from all classical considerations of multiparticle production.

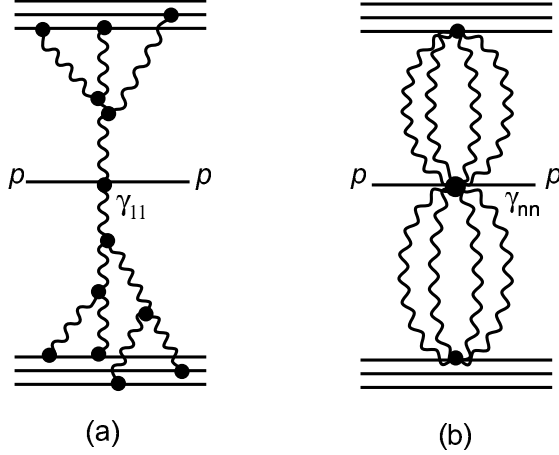


Figure 8: Multipomeron diagrams for inclusive production: (a) - diagrams with fusion and splitting of parton chains; (b) - diagrams with rescattering of n parton chains.

7 Numerical estimates

Let us present examples of numerical estimates of elliptic flow for the exponential parametrization (6) of the inclusive vertex. They are illustrative only. We intentionally do not fit experimental data because, first, little quantitative information on the inclusive vertex γ exists and, second, it is necessary to have more reliable model for nuclear multipomeron effects. In this publication we aim to demonstrate that qualitative features of elliptic and directed flows peculiar to the mechanism under discussion are in agreement with experimental observations. In particular, as it is seen from Eq. (21) the value of $v_2(p_t, b)$ grows with increase of both transverse momentum p_t and impact parameter b .

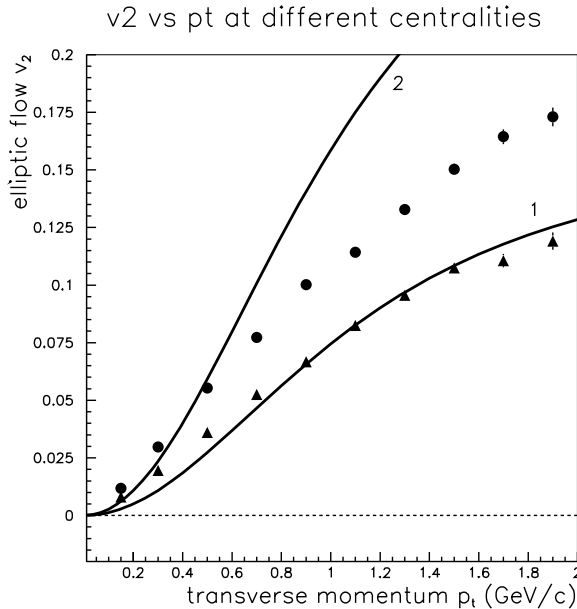


Figure 9: Elliptic flow v_2 as a function of transverse momentum p_t in $Au - Au$ collisions for two centrality values: $C = 13\%$ ($b \sim 5.6$ fm) – curve 1; $C = 27.5\%$ ($b \sim 7.9$ fm) – curve 2.

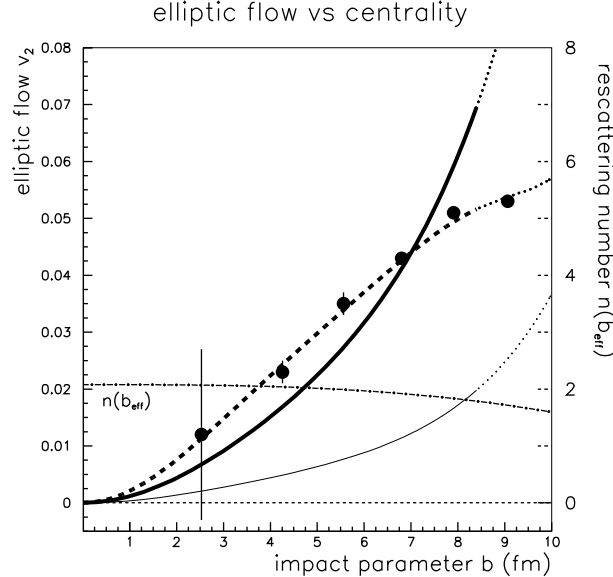


Figure 10: Elliptic flow v_2 as a function of impact parameter b at $p_t = 0.5 \text{ GeV}/c$. Calculations for $b > 8 \text{ fm}$ are shown with dotted curve. Thick solid line corresponds to calculations at $\epsilon = 0.4$. Thin solid line corresponds to calculations at $\epsilon = 0.1$, and dotted line – at $\epsilon = 0.1$ multiplied to the mean rescattering number squared $n(b_{eff}) = n(0.65b)$. The dashdotted line at this picture gives $n(b_{eff})$ as a function of b (the right scale).

It is shown on Fig.9 p_t -dependence of elliptic flow for two values of centrality. Calculations were made for two different values of centrality at $\epsilon = 0.4$ for the standard Woods-Saxon parameterization of nuclear density. Note that for large p_t the growth of v_2 is stopped due to higher order of ϵ though it is not quite justified to use Eq.(6) in high p_t region. Experimental data are taken from [11]. The too fast increase of theoretical predictions with centrality may be related to a neglect of multipomeron diagram contribution (see below).

Fig.10 presents the b -dependence of elliptic flow. According to Eq. (21) v_2 grows as b^2 (thick solid line, $\epsilon = 0.4$) in contradiction with the experimental behavior at very large b when nuclei only touch each other. Let us note here that in the case of very large impact parameter values where nuclear densities are quite small an accuracy of the model is low. This is why calculation results for $b > 8 \text{ fm}$ are shown with dotted curves. The dashed curve corresponds to the simplest account of nuclear effects due to inter-pomeron interactions – calculations at smaller parameter value $\epsilon = 0.1$ (thin solid line) are multiplied to the factor $n(b_{eff})^2$. The function $n(b_{eff})$ gives an effective number of interacting pomeron fluctuations⁹. It is also presented at the figure (dash-dotted line) and one can see that the maximal number of pomeron interaction is about 2 for central collisions. Experimental data are from [11].

Dependence of the directed flow v_1 on rapidity y calculated at $\delta = 0.1$ for two energies (200 and 64 GeV) is presented on Fig. 11. It is antisymmetric and concentrated at the edges of the rapidity interval rapidly decreasing to the middle of it. The experimental data corresponding to centrality 30 - 60 % are taken from ref.[12].

⁹ The function $n(b)$ was estimated in the eikonal approximation with effective parton-nucleon cross section value $\sigma \sim 10 \text{ mb}$. The mean position of interacting nucleon in a nucleus was taken as $b_{eff} = 0.65b$.

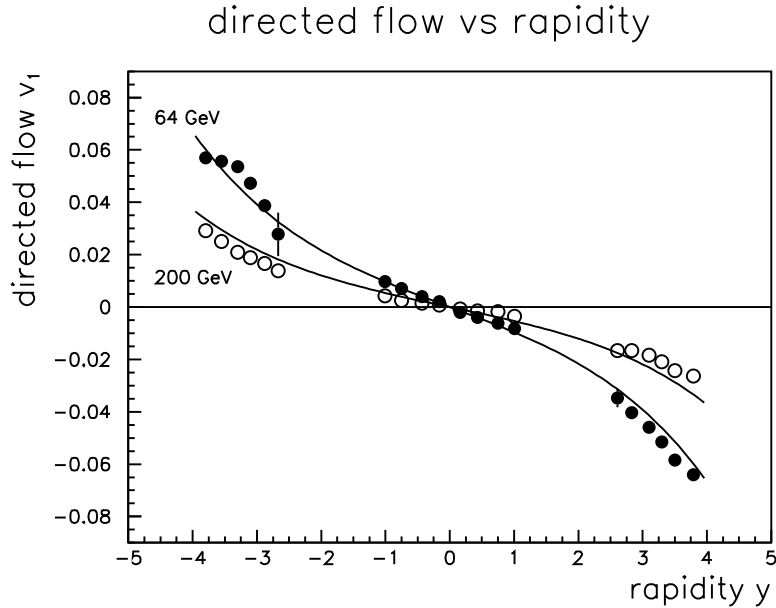


Figure 11: Directed flow v_1 as a function of rapidity y .

8 Conclusions

The main aim of this paper is to draw attention to the mechanism of appearance of azimuthal correlations between produced particles related to specific parton correlations in initial states of colliding nuclei, and which is not caused by particle interactions in the final state.

The mechanism under discussion is connected with correlation between parton transverse momentum and its transverse position inside nucleus. Transverse momenta of partons in incoming nuclei (before collision) are already partially aligned along transverse nuclear radiuses. The non-central collision of nuclei selects the asymmetric overlapping part of the fast nucleus resulting in $\mathbf{p}_t - \mathbf{b}$ correlations for produced particles.

We discussed this phenomenon using the simplest reggeon diagram in order to emphasize the fact of its existence. For quantitative description of asymmetries it is necessary to account for a more complicated mechanism related to interactions between different chains. We emphasized that this mechanism can substantially increase elliptic flow and modify its atomic number dependence. Role of multipomeron interactions describing these effects increases with energy and is important at RHIC energies. This mechanism influences dependence of asymmetries on centrality, transverse momenta and rapidity.

Evidently the final state interaction can also contribute to azimuthal asymmetry of produced particles. In order to obtain an information on properties of hadronic matter at high temperatures and densities it is crucial to separate effects due to initial and final state interactions. In particular it is important to carry out a detailed investigation of azimuthal correlations of particles produced in nucleon-nucleon and nucleon-nucleus interactions. Such studies will be possible in high-multiplicity events at LHC.

Acknowledgements. We are grateful to L.V. Bravina, Yu.A. Simonov and E.E. Zabrodin for stimulating interest and discussions. The work was supported by RFBR grants 06-02-17012, 08-02-00677, 06-02-72041-MNTI, and SSh 843.2006.2.

References

- [1] J.-Y. Ollitrault, Phys. Rev. D **46**, 229 (1992).
- [2] J.-Y. Ollitrault, Phys. Rev. D **48**, 1132 (1993).
- [3] S. Voloshin, Y. Zhang, Z. Phys. C **70** (1996) 665.
- [4] H. Sorge, Phys. Rev. Lett. **78**, 2309 (1997).
- [5] S.A. Voloshin, Nuclear Physics A, **715**, 379 (2003).
- [6] S. S. Adler *et al.*, PHENIX Collaboration, Phys. Rev. Lett. **91**,182301 (2003).
- [7] M. Tonjes (for the PHOBOS Collaboration), J. Phys. G. **30**, S1225 (2004).
- [8] J. Adams *et al.*, STAR Collaboration, Phys. Rev.C **72**, 014904 (2005).
- [9] V.A. Abramovsky, V.N. Gribov, O.V. Kancheli, Yad. Fiz. **18**, 595 (1973),
Sov. J. Nucl. Phys. **18**, 308 (1974).
- [10] A.B. Kaidalov, Phys. Usp. **46**, 1121 (2003), Usp. Fiz. Nauk **46**, 1153 (2003).
- [11] STAR collaboration, Phys. Rev. C **66**, 034904 (2002).
- [12] STAR collaboration, nucl-ex/0807.1518.